A mechanical property evaluation of Ti6Al4V cellular lattice structures fabricated by selective laser melting

IOP Conf. Series: Materials Science and Engineering **788** (2020) 012010 doi:10.1088/1757-899X/788/1/012010

A mechanical property evaluation of Ti6Al4V cellular lattice structures fabricated by selective laser melting

M Z Azir[1], W S W Harun[2,*] and K Kadirgama[2]

[1]Faculty of Engineering Technology, DRB Hicom University of Automotive Malaysia, 26600 Pekan, Pahang, Malaysia

[2]Faculty of Mechanical & Manufacturing Engineering, Universiti Malaysia Pahang, 26600 Pekan, Pahang, Malaysia.

[*]Corresponding author: sharuzi@ump.edu.my

Abstract. Cellular structures are similarly identified as lattice structures or foam structures which are commonly constructed of ligaments. Cellular structures exist widely in nature, such as the coral, honeycomb, and the natural bones. Cellular structures are also manufactured and used in various applications such as honeycomb bumper structures and truss bridge. Ti6Al4V is one of the most commonly used titanium alloy and is applied in a wide range of application where low density very good corrosion resistance are necessary such as direct manufacturing of part and prototypes for racing and aerospace industry, biomechanical application such as implants and prosthesis, marine application, chemical industry, and gas turbine. This paper investigates the mechanical properties of Ti6Al4V lattice structures fabricated by additive manufacturing, also known as 3D printing. The samples are fabricated by selective laser melting (SLM) using titanium alloy (TI6Al4V). Four factors were selected to determine its influence on the Young's modulus and compressive strength, which is strut size, strut shape, unit cell size, and porosity. All the samples categorize to six groups by its design volume porosity obtained from CAD file. Solidwork design software was used in this study. The influence was shown in a comparison graph. Detailed characterizations of compression test were conducted and reported. The built structures have a Young's modulus ranging between 0.01 and 1.84 Gpa. Porosity was realized to play an important role in determining the Young's modulus and compressive strength.

Keywords. Additive manufacturing; SLM; Lattice structure; Ti6Al4V; Mechanical testing.

1. Introduction

Additive manufacturing (AM) is known as the process of joining materials to make objects from 3D model data, normally layer by layer, as contrasting to traditional machining [1]. AM is able to deliver parts of very complex and complicated geometries with a minimum need for post-processing. For example in moulding, finishing or post-processing is required to get the best quality of end product. AM is a tool that can increased 'design freedom' and give opportunity to designers and engineers to invent unique products that can be manufactured in low volume at lower cost. Selective laser melting (SLM) of metal powders is one of additive manufacturing technology with the ability of layer by layer building method of complex shape to develop functional parts. SLM also known as 3D printing, technique that uses a laser power source to fuse powder materials to form working parts directly based

on computer aided design (CAD) files. Titanium alloy open cellular structures are highly in demand for many applications such as lightweight aerospace products, automotive, and medical applications. Traditional manufacturing methods such as casting, however, faces difficulty in making titanium alloy open cellular structures with differently designed unit cell size, strut size, strut shape, and volume fraction. This study investigates the mechanical properties of Ti6Al4V open cellular structures fabricated by selective laser melting process (SLM). Titanium alloy is specifically chosen for this application as they are highly resistance to corrosion, biocompatible, and have high specific strength.

Nowadays, the research on Ti6Al4V has been concentrated on using them to develop sophisticated orthopaedic implant [2-7]. Harrysson, et al. [3] and Hazlehurst, et al. [4] used EBM/Ti-6Al-4V and SLM/CoCrMo, individually, to deliver permeable femoral stems. Harrysson et al. [3] chose a rhombic dodecahedron grid structure with a cell size of 3 mm to develop the body of the permeable stem. While, Hazlehurst et al. [4] develops the permeable body by choosing a cubic cross-section structure encompassed by a dense external shell. Both of these approaches have reduced the weight of stem by 44–48% and flexural stiffness by 57–60% compared with their dense counterparts. Apart from that, since Ti6Al4V is preferably fabricated using SLM, most of the research has also been concentrated on studying the mechanical properties and failure mechanism[8] of the structure develop through the SLM process.

From the previous research, it was stated that the properties of the component are ultimately dependent on the strut size and no notable shortcoming in the associating layers of the structures is observed when subjected to shearing powers. Min et al. [9] had performed the pressure weakness testing on titanium combination cell structures and witnessed the weariness quality expanded with an expanding relative thickness and cyclic tightening of the struts inside the cell structure, which is the cause for failure. Spoerke et al. [10] reported that the fatigue strength and energy absorption of titanium structures fabricated by the SLM could be enhanced by performing a warm treatment. He also proposed several regions that could be further strengthened to make equivalent load dissemination inside the structure. Morlock et al. [11] investigated the mechanical properties of an open cell CoCrMo structure with a pore size of 0.5 mm and reported the structure to have comparable mechanical properties to monetarily fabricated components using elective composites. Furthermore, his recent findings have shown that square pore CoCrMo cell structures fabricated utilizing SLM offers compressive properties similar to human bone [12].

Thus, this paper shows the mechanical properties such as Young's modulus and yield stress of different cross-section structures builded from Ti6AL4V using SLM. Four processing parameter was considered in this study namely, strut size, strut shape, unit cell, and porosity. The compression test was executed to determine the highest influential parameters toward the responses (Young's modulus and yield stress). The optimization of the parameters values to produce structure near to human bone properties is also discussed in the paper.

2. Material and experimental set up

2.1. Material

Ti6Al4V powder with a mean particle size of 30 μm is used in this research. The powder quality is imperative to lessen the substance of debasements (oxygen, hydrogen, and nitrogen), which may influence mechanical properties of laser-sintered parts. The compositions of Ti6Al4V powder used in this study are shown in table 1. In this work, the sample was fabricated with an open cellular structure with four controlled parameters which is, unit cell size, strut size, strut shape, and porosity.

2.2. Fabrication of lattice samples

The lattice structure sample is fabricated using the EOSINT M270 adapting the laser-sintering framework with improved parameters to acquire the full thickness of laser-sintered parts. All of the samples were successfully built with using selective laser melting process as shown in figure 1. The

optimum machine setting parameter that applied is shown in table 2. The sample parameters were divided into three levels, which is min, medium, and max as shown in table 3.

Table 1. Composition of the Ti6Al4V powder.

Element	%
Aluminium	6.75
Vanadium	4.50
Carbon	0.08
Nitrogen	0.05
Oxygen	0.2
Hydrogen	0.0125
Iron	0.3
Yttrium	0.005
Other	0.1
Titanium	Remainder

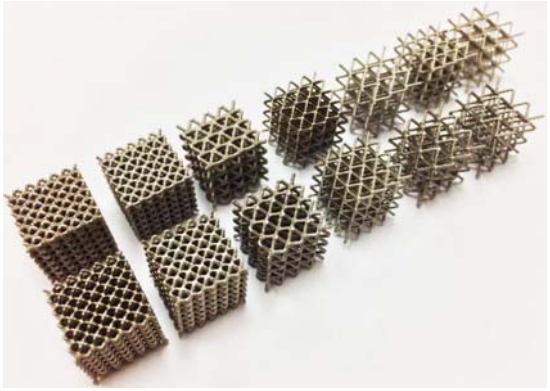

Figure 1. The open cellular structure sample in this study.

Table 2. SLM machine setting parameter.

Layer thickness	50μm
Build chamber preheating	150°c
Scale factor	1.0011
Laser power (outer hull)	275watt
Scanning speed	760mm/s
Laser power (fill contours)	175watt
Scanning speed	500mm/s
Hatching distances	0.08mm

Table 3. Sample parameters.

No.	Parameters	Min.	Medium	Max.
1	Unit Cell Size (mm^3)	2 ×2×2	3 ×3×3	4 ×4×4
2	Strut Size (mm)	0.55	0.60	0.70
3	Strut Shape	Hexagon	Circle	Rectangular
4	Designed Volume Porosity (%)	70/75	80/85	90/95

Figure 2 shows the strut designs that were drawn using CAD software. Based on the design, their volume porosity is determined to be 70, 75, 80, 85, 90, and 95%, respectively. Total numbers of samples fabricated is 13 with 5 replications for each parameter. The entire material preparations by four processing controlled parameters is shown in table 4. Design of experiments is used to develop the experiment table.

(a)

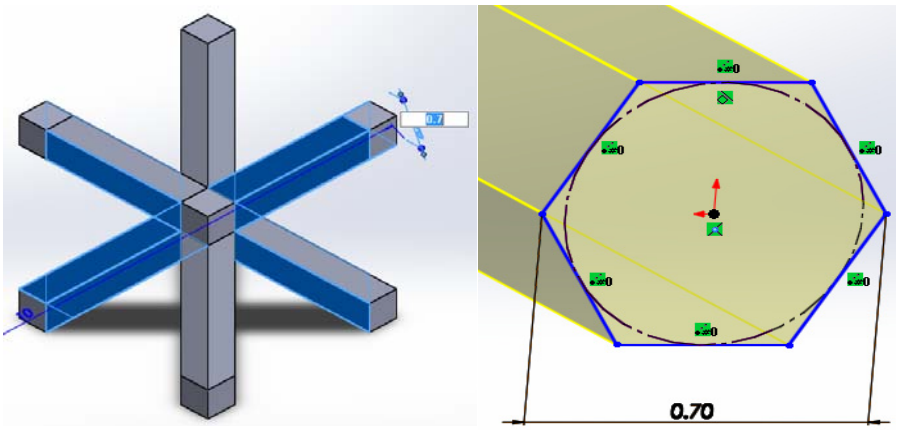

(b)

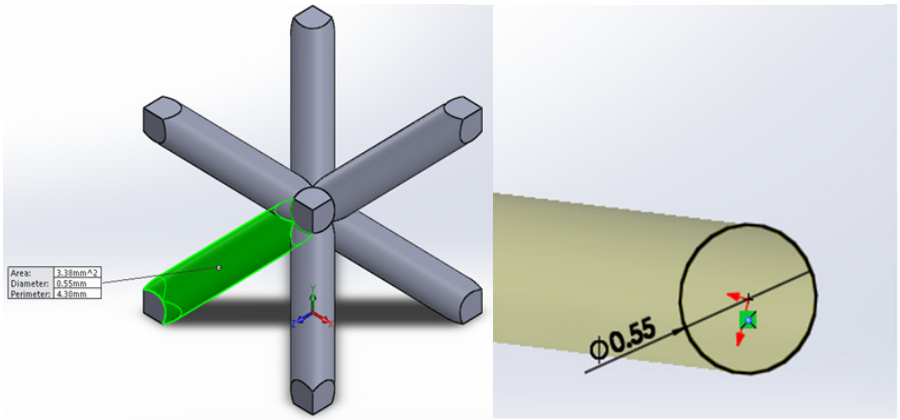

(c)

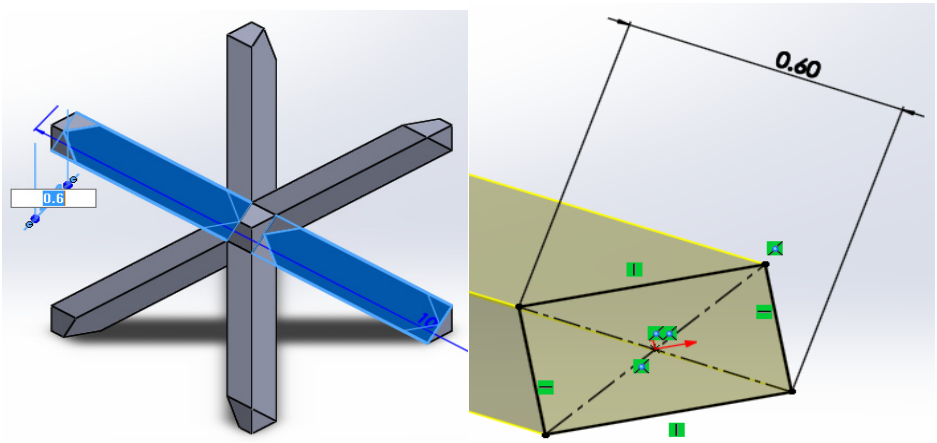

Figure 2. (a) Strut 0.7 mm, hexagon; (b) strut 0.55 mm, circle; (c) strut 0.6 mm, square.

Table 4. Material preparations by four processing parameter.

The DOE table unit cell (mm^3)	Strut size (mm)	Strut shape	Porosity (%)	Design volume (%)
8	0.6	H	70	69.4
8	0.7	C	70	64.3
8	0.7	S	70	72.4
27	0.7	C	75	76.6
27	0.7	H	80	80.2
8	0.55	S	80	81.8
27	0.55	H	85	87.14
27	0.55	C	85	84.7
64	0.6	H	90	91.1
64	0.6	C	90	89.4
64	0.7	S	90	91.9
27	0.6	S	90	89.7
27	0.6	S	90	89.7
27	0.6	S	90	89.7
64	0.55	S	95	94.9

The fabricated samples was divided into six different groups based on their designed volume porosity: 70, 75, 80, 85, 90, and 95%. Designed volume porosity was defined as the percentage of hollow area introduced in the lattice structure compared with the volume fraction of the solid strut. Volume for solid cube with dimension of 12 mm × 12 mm × 12 mm is 1728 mm^3 as simulated in the CAD software. Hence, the volume porosity was obtained by subtracting the solid cube volume with the volume fraction of the produced porous structure. The selection of the stated designed volume porosity was based on the average porosity of actual femoral bone structural, which is between 70 %

and 95%. Among all four parameters studied, the amount of porosity in sample was the most influencing factor that determines the stiffness of the sample. The stiffness can be measured by the elastic modulus or also known as Young's modulus. The Young's modulus was a measurement of a mechanical property of linear elastic materials.

To obtain Young's modulus value for the sample, the relationship between stress and strain of the sample must be systematically defined. The size of the cell for all samples was constant regardless of the difference in the designed volume porosities.

A set of parameters was prepared for the complex structure of the open cellular structure. In fact, based on design volume porosity data, the porosity is observed to differ for each sample (cell size) since the different strut shape with the same strut dimension produces different porosity and vice versa. The unit cell size determines the pore size of the cellular structure. The larger unit cell size ($4 \times 4 \times 4$ mm^3) offers the most significant size of interconnected pores which is around 3 mm in diameter. Two-millimetre diameter pore size was obtained on the medium unit cell size of $3 \times 3 \times 3$ mm3. Whereas, the smallest unit cell size gives the smallest pore size in this study which is 1 mm diameter. The excellent characteristic of the implants is high porosity, appropriate pore size (0.5 to 3 mm), rough surface, and pore interconnectivity. These features promote a friendly physical environment for tissue ingrowth which later improves the level of implant fixation to the bone.

The mechanical property of these inserts is usually three to five times higher than those produced by other means and the likelihood of irritation caused by micro-debris that breaks amid the system also decreased. Commonly, a porosity of 75–85% and a pore size of more than 100 μm are preferred for fast bone ingrowth. The amount of pore on the strut is almost constant regardless of the sample conditions. The amount of pore on the strut is between 5 and 10%.

2.3. Compression test

The stiffness of the open cellular structure sample will be presented in by Young's modulus values. The Young's modulus represents the modulus of elasticity which indicates the rigidity of the sample. A study was done by Nazarian, et al. [13] and Rohlmann, et al. [14] on the actual human femur trabecular bone found that Young's modulus range of falls between 0.32 to 0.40 GPa. The sample with cellular structures was built using an SLM250HL machine (SLM Solutions GmbH). The compression tests were performed using a Shimadzu Testing System (VHS8800) with a low rate method. The maximum loading capacity of the machine is 100 kN, stroke rate 0.1mm/minute, meshing 0.1, and step 25. The load history was measured by a Kistler load cell 9071A. The displacement history was measured by an internal linear variable differential transformer with data filter by setting cut off frequency of 1000 Hz. The deformation process was also recorded by a camera within an interval of 30 s. The examples are put on the base pressure plate which is situated at an extensive separation from the best plate toward the start of every pressure test. In any case, it ought to be noticed that the grinding impact on the uniaxial level anxiety isn't so huge for crushable cell materials, on the grounds that the Poisson's proportion amid the pressure in level area of a specimen is near zero. This quality relates at the most extreme anxiety that the structure can bolster before crumple. Kept stacking brought about a plastic fall until breaking and densification. The level of softening is by all accounts more influenced by porosity. For impact energy absorption applications, a stress versus strain response with little or no softening after yield is desirable [15, 16].

3. Results and discussion

Figure 3 shown the amount of porosity has significantly affected the behaviour of the stress-strain properties of the sample. Lower amount of porosities; 70, 75, & 80% showed higher stress which later can be translated into the higher value of Young's Modulus. Higher young's modulus means higher stiffness. Or else, the samples with higher amount of porosity demonstrated lower value of Young's modulus which explained into lower stiffness. The effects of porosity amount to yield stress value is shown in table 5. The summary of the young's modulus value is shown in table 6. Each stress-strain curve can be divided into three main phases; Elastic deformation, shear deformation, and Collapse.

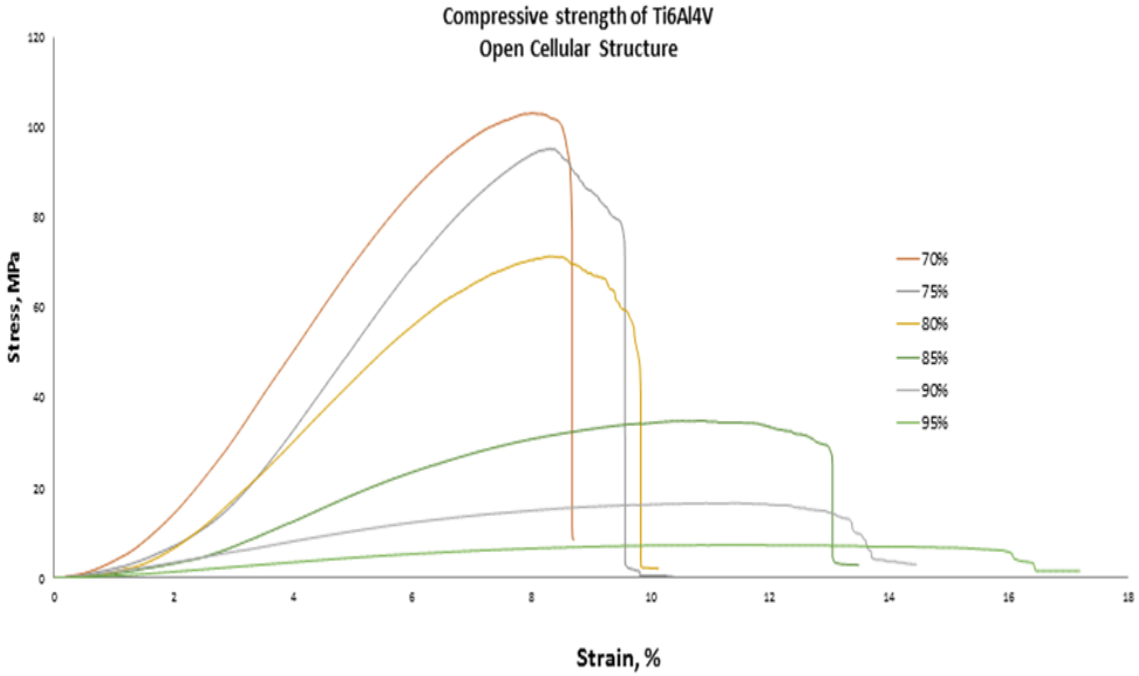

Figure 3. Compressive stress-strain curve of an as-built open cellular structure samples.

Table 5. Effects of porosity to yield stress.

Porosity (%)	Yield stress (Mpa)
70	88
75	23
80	58
85	24.3
90	25.5
95	5.4

Table 6. Summary of the young's modulus value.

Volume Porosity (%)	Young's Modulus (GPa)	Remarks
70	1.84	Close to the value of Young's Modulus of actual femoral trabecular bone (0.1 to 0.4 GPa)
75	1.83	
80	1.36	
85	0.57	
90	0.22	
95	0.01	

Most of the patients with fracture hip experience difficulty in doing their routine activities. Consequently, they require hip replacement or arthroplasty to solve this difficulty [17]. A hip replacement is a procedure of replacing the diseased hip joint with a new artificial part called prosthesis. It is used to transfer load from the acetabulum to the femur through a metal stem that is inserted into the femur [18]. This procedure is aimed to improve the mobility but it's still having a problem if the Young's Modulus value of the artificial hip or implant differs and not optimum to the real bone. It's occurring when some of the loads are taken by implant and shielded from going to the bone.

3.1. Compressive stress - strain

As shown in figure 3, all samples at different porosity demonstrated these regions clearly. However, what makes the different the samples is the width of the each region. The sample with lower amount of porosity demonstrated bigger region of elastic deformation and smaller region of shear deformation before collapse. Whereas, 16 higher porosity samples show opposite which is smaller elastic region and bigger for shear deformation region as shown in figure 4 and figure 5. The materials used in each component of the hip implant must have suitable properties to allow them to replace the natural tissue and continue to perform the same functions.

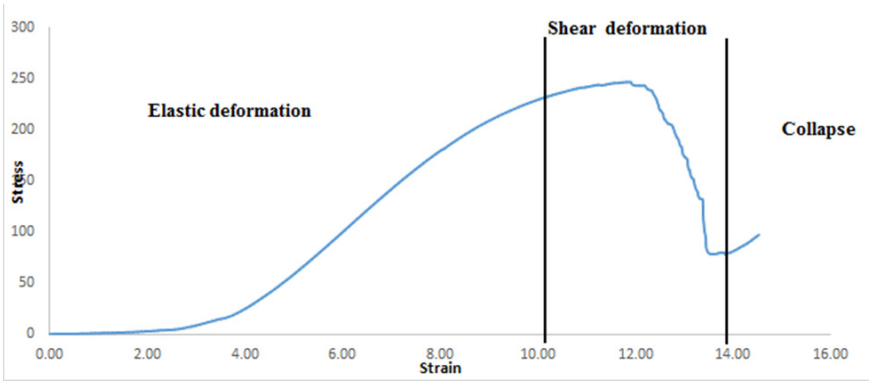

Figure 4. Compression stress-strain curve of an as built open cellular structure sample with 70 percent volume porosity.

The mechanical property requirement for the femoral stem is primarily to support the loads that are applied, and therefore the modulus of the implant material is one of the main criteria. The femoral head and acetabular cup components are required to act as bearing surfaces, and therefore, the coefficient of friction and wear rates of these materials will be important. For biomedical applications like implants, typical metallic materials used in SLM have higher modulus than natural bones. Modulus mismatch can cause an adverse effect called "stress shielding "[19]. The femoral stem component replaces a large portion of bone in the femur, and this is therefore the load-bearing part of the implant. To bear this load, it must have a Young's Modulus comparable to that of cortical bone. If the implant is not as stiff as bone, then the remaining bone surrounding the implant will be put under increased stress. If the implant is much stiffer than the bone, then the implant will bear more of the load. Because the bone is shielded from much of the stress being applied to the femur, the body will respond to this by increasing osteoclast activity, causing bone resorption.

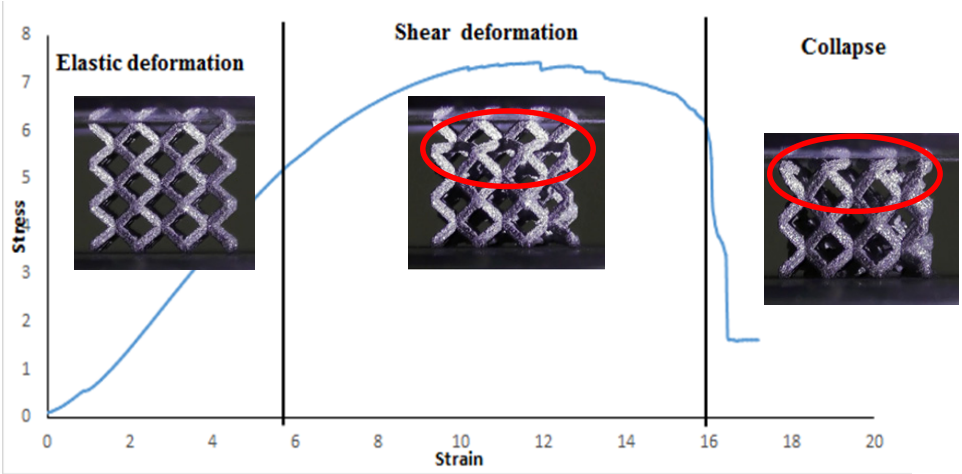

Figure 5. Compression stress-strain curve of an as built open cellular structure sample with 95 percent volume porosity.

3.2. Deformation of lattice structure

The deformation of lattice structure was recorded during compression test as shown in figure 6. For this sample the compressive stress resulting the deformation on top area of strut. For cell size with lower porosity, higher stress that needed to collapse the strut is up to 200 MPa. While, for the higher porosity lower stress is needed to collapse the cell size. Energy absorption capacity is one of the key indicators in the characterization of lattice structure materials for impact resistance and energy absorption applications [20].

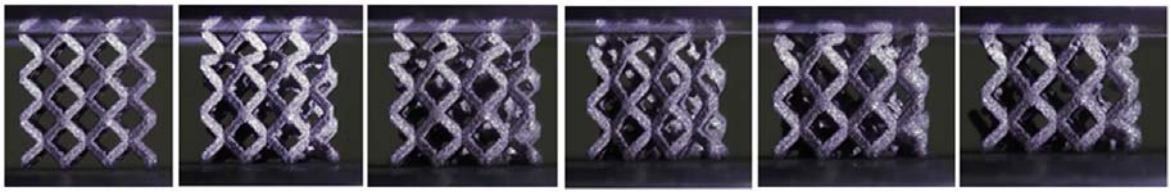

Figure 6. Deformation video frames from the compression of Ti6Al4V samples.

3.3. Optimum structure parameter for implant

The optimization of the processing parameter factors for optimum Young's modulus of actual femoral trabecular bone (0.1 to 0.4 GPa) is a crucial part. The optimization criteria selected a lower boundary of 0.1 GPa and upper boundary of 0.5Gpa. The target values are 0.4 GPa. It shows that the optimum structure parameters that are produce near the 0.4 GPa are the unit cell of 4×4×4, strut size of 0.7 mm, porosity of 91%, and strut shape of Hexagon. The desirability is nearly 1 (0.9364), and this satisfies the goal of the optimization. Implant materials must be biocompatible with body tissues and fluids, corrosion resistant, and mechanically compatible with interfacing replacement/body components. It must produce a minimum degree of rejection. Products resulting from reaction with body fluids must be tolerated by the surrounding body tissues such that normal tissue function is unimpaired. Biocompatibility is a function of the location of the implant, as well as its chemistry and shape [21].

4. Conclusions

In this investigation, the aim has achieved to assess the mechanical properties of Ti6Al4V cellular lattice structure. The result shows that Young's modulus and compressive strength from compression test influenced by four factors which is strut size strut shape, cell size, and porosity. Sample with lower amount of porosity revealed bigger region of elastic deformation and smaller region of shear deformation before collapse. While, the sample with higher volume porosity show the vice versa, smaller elastic region and bigger for shear deformation before collapse.

Acknowledgement

This research was established by funding of the NPRP grant NPRP 8-876-2-375 from the Qatar National Research Fund (a member of Qatar Foundation).

References

[1] Kadirgama K, Harun W S W, Tarlochan F, Samykano M, Ramasamy D, Azir M Z and Mehboob H 2018 Statistical and optimize of lattice structures with selective laser melting (SLM) of Ti6AL4V material *The International Journal of Advanced Manufacturing Technology* **97** 495-510

[2] Bandyopadhyay A, Krishna B V, Xue W and Bose S 2009 Application of laser engineered net shaping (LENS) to manufacture porous and functionally graded structures for load bearing implants *Journal of Materials Science: Materials in Medicine* **20** 29

[3] Harrysson O L, Cansizoglu O, Marcellin-Little D J, Cormier D R and West H A 2008 Direct metal fabrication of titanium implants with tailored materials and mechanical properties using electron beam melting technology *Materials Science and Engineering: C* **28** 366-73

[4] Hazlehurst K B, Wang C J and Stanford M 2014 An investigation into the flexural characteristics of functionally graded cobalt chrome femoral stems manufactured using selective laser melting *Materials & Design* **60** 177-83

[5] Murr L, Gaytan S, Medina F, Lopez H, Martinez E, Machado B, Hernandez D, Martinez L, Lopez M and Wicker R 2010 Next-generation biomedical implants using additive manufacturing of complex, cellular and functional mesh arrays *Philosophical Transactions of the Royal Society A: Mathematical, Physical and Engineering Sciences* **368** 1999-2032

[6] Harun W, Asri R, Alias J, Zulkifli F, Kadirgama K, Ghani S and Shariffuddin J 2018 A comprehensive review of hydroxyapatite-based coatings adhesion on metallic biomaterials *Ceramics International* **44** 1250-68

[7] Harun W, Manam N, Kamariah M, Sharif S, Zulkifly A, Ahmad I and Miura H 2018 A review of powdered additive manufacturing techniques for Ti-6Al-4V biomedical applications *Powder Technology* **331** 74-97

[8] Leong K, Cheah C and Chua C 2003 Solid freeform fabrication of three-dimensional scaffolds for engineering replacement tissues and organs *Biomaterials* **24** 2363-78

[9] Min B-M, Lee G, Kim S H, Nam Y S, Lee T S and Park W H 2004 Electrospinning of silk fibroin nanofibers and its effect on the adhesion and spreading of normal human keratinocytes and fibroblasts in vitro *Biomaterials* **25** 1289-97

[10] Spoerke E D, Murray N G, Li H, Brinson L C, Dunand D C and Stupp S I 2005 A bioactive titanium foam scaffold for bone repair *Acta Biomaterialia* **1** 523-33

[11] Morlock M, Schneider E, Bluhm A, Vollmer M, Bergmann G, Müller V and Honl M 2001 Duration and frequency of every day activities in total hip patients *Journal of biomechanics* **34** 873-81

[12] Ahmadi S, Yavari S, Wauthle R, Pouran B, Schrooten J, Weinans H and Zadpoor A 2015 Additively manufactured open-cell porous biomaterials made from six different space-filling unit cells: The mechanical and morphological properties *Materials* **8** 1871-96

[13] Nazarian A, Muller J, Zurakowski D, Müller R and Snyder B D 2007 Densitometric, morphometric and mechanical distributions in the human proximal femur *Journal of biomechanics* **40** 2573-9

[14] Rohlmann A, Zander T, Schmidt H, Wilke H-J and Bergmann G 2006 Analysis of the influence of disc degeneration on the mechanical behaviour of a lumbar motion segment using the finite element method *Journal of biomechanics* **39** 2484-90
[15] Kooistra G W, Deshpande V S and Wadley H N 2004 Compressive behavior of age hardenable tetrahedral lattice truss structures made from aluminium *Acta Materialia* **52** 4229-37
[16] Ashby M F, Evans T, Fleck N A, Hutchinson J, Wadley H and Gibson L 2000 *Metal foams: a design guide*: Elsevier)
[17] Lieberman J R, Thomas B J, Finerman G A and Dorey F 2003 Patients' reasons for undergoing total hip arthroplasty can change over time *The Journal of arthroplasty* **18** 63-8
[18] Terrier A 1999 Adaptation of bone to mechanical stress: theoretical model, experimental identification and orthopedic applications. Verlag nicht ermittelbar)
[19] Traini T, Mangano C, Sammons R, Mangano F, Macchi A and Piattelli A 2008 Direct laser metal sintering as a new approach to fabrication of an isoelastic functionally graded material for manufacture of porous titanium dental implants *Dental materials* **24** 1525-33
[20] Li Q, Magkiriadis I and Harrigan J J 2006 Compressive strain at the onset of densification of cellular solids *Journal of cellular plastics* **42** 371-92
[21] Black J and Hastings G 2013 *Handbook of biomaterial properties*: Springer Science & Business Media)